Apathy in patients with cerebral amyloid angiopathy: a multimodal neuroimaging study

Chokesuwattanaskul, Anthipa; Zanon Zotin, Maria Clara; Schoemaker, Dorothée; Sveikata, Lukas; Gurol, M Edip; Greenberg, Steven M; Viswanathan, Anand

How to cite

CHOKESUWATTANASKUL, Anthipa et al. Apathy in patients with cerebral amyloid angiopathy: a multimodal neuroimaging study. In: Neurology, 2023, vol. 100, n° 19, p. e2007–e2016. doi: 10.1212/WNL.0000000000207200

This publication URL: https://archive-ouverte.unige.ch/unige:171827

Publication DOI: 10.1212/WNL.0000000000207200

Published Ahead of Print on March 20, 2023 as 10.1212/WNL.0000000000207200

Neurology®
The most widely read and highly cited peer-reviewed neurology journal
The Official Journal of the American Academy of Neurology

AMERICAN ACADEMY OF NEUROLOGY®

Neurology Publish Ahead of Print
DOI:10.1212/WNL.0000000000207200

Apathy in Patients With Cerebral Amyloid Angiopathy: A Multimodal Neuroimaging Study

Author(s):
Anthipa Chokesuwattanaskul, M.D.[1, 2, 3]; Maria Clara Zanon Zotin, M.D.[1,4]; Dorothée Schoemaker, Ph.D[1]; Lukas Sveikata, M.D.[1,5]; M. Edip Gurol, MD MSc[1]; Steven M Greenberg, MD, PhD[1]; Anand Viswanathan, MD PhD[1]

Corresponding Author:
Anthipa Chokesuwattanaskul, anthipa.c@chula.ac.th

Affiliation Information for All Authors: 1. J. Philip Kistler Stroke Research Center, Department of Neurology, Massachusetts General Hospital, Harvard Medical School, Boston, Massachusetts, United States; 2. Division of Neurology, King Chulalongkorn Memorial Hospital, Thai Red Cross Society, Bangkok, Thailand; 3. Cognitive Clinical and Computational Neuroscience Research Unit, Faculty of Medicine, Chulalongkorn University, Bangkok, Thailand; 4. Center for Imaging Sciences and Medical Physics, Department of Medical Imaging, Hematology and Clinical Oncology. Ribeirão Preto Medical School, University of São Paulo, Ribeirão Preto, SP, Brazil; 5. Division of Neurology, Department of Clinical Neurosciences, Geneva University Hospital, Faculty of Medicine, University of Geneva, Geneva, Switzerland.

Equal Author Contribution:

Contributions:
Anthipa Chokesuwattanaskul: Drafting/revision of the manuscript for content, including medical writing for content; Major role in the acquisition of data; Study concept or design; Analysis or interpretation of data
Maria Clara Zanon Zotin: Drafting/revision of the manuscript for content, including medical writing for content; Major role in the acquisition of data; Study concept or design; Analysis or interpretation of data
Dorothée Schoemaker: Drafting/revision of the manuscript for content, including medical writing for content; Major role in the acquisition of data; Analysis or interpretation of data
Lukas Sveikata: Drafting/revision of the manuscript for content, including medical writing for content; Major role in the acquisition of data
M. Edip Gurol: Drafting/revision of the manuscript for content, including medical writing for content
Steven M Greenberg: Drafting/revision of the manuscript for content, including medical writing for content
Anand Viswanathan: Drafting/revision of the manuscript for content, including medical writing for content; Study concept or design; Analysis or interpretation of data

Figure Count:
2

Table Count:
2

Search Terms:
[2] All Cerebrovascular disease/Stroke, [32] Vascular dementia, [120] MRI, [121] fMRI, [199] All Neuropsychology/Behavior

Acknowledgment:

Study Funding:
This study was supported by the following NIH grants: R01AG047975, R01AG026484, P50AG005134, K23AG02872605. L.S. was supported by the Swiss National Science Foundation (P2GEP3_191584).

Disclosures:
All authors report no disclosures relevant to the manuscript.

Preprint DOI:

Received Date:
2022-08-15

Accepted Date:
2023-02-03

Handling Editor Statement:
Submitted and externally peer reviewed. The handling editor was Associate Editor Linda Hershey, MD, PhD, FAAN.

Abstract

Objective

To analyze the prevalence and associated clinical characteristics of apathy in sporadic cerebral amyloid angiopathy and investigate whether apathy was associated with disease burden and disconnections of key structures in the reward circuit through a structural and functional multi-modal neuroimaging approach.

Methods

Thirty-seven probable sporadic cerebral amyloid angiopathy participants without symptomatic intracranial hemorrhage or dementia (mean age, 73.3 ± 7.2, % male = 59.5%) underwent a detailed neuropsychological evaluation, including measures of apathy and depression, and a multimodal MR neuroimaging study. A multiple linear regression analysis was used to assess the association of apathy with conventional small vessel disease neuroimaging markers. A voxel-based morphometry with a small volume correction within

regions previously associated with apathy and a whole-brain tract-based spatial statistics were done to identify differences in the gray matter and white matter between the apathetic and the non-apathetic groups. Gray matter regions significantly associated with apathy were further evaluated for their functional alterations as seeds in the seed-based resting-state functional connectivity analysis. Potential confounders, namely, age, gender, and measures of depression were entered as covariates in all analyses.

Results

A higher composite small vessel disease marker score (CAA-SVD) was associated with a higher degree of apathy (standardized coefficient = 1.35 (0.07 – 2.62), adjusted R^2 = 27.90, p = 0.04). Lower gray matter volume of the bilateral orbitofrontal cortices was observed in the apathetic group than the non-apathetic group (F = 13.20, family-wise error corrected p = 0.028). The apathetic group demonstrated a widespread decrease in white matter microstructural integrity compared to the non-apathetic group. These tracts connect key regions within and between related reward circuits. Finally, there was no significant functional alterations between the apathetic and the non-apathetic groups.

Conclusions

Our findings revealed the orbitofrontal cortex as a key region in the reward circuit associated with apathy in sporadic cerebral amyloid angiopathy, independent from depression. Apathy was shown to be associated with a higher CAA-SVD score and an extensive disruption of white matter tracts, which suggested that a higher burden of CAA pathology and the disruption in large-scale white matter networks may underlie manifestations of apathy.

Introduction

Sporadic cerebral amyloid angiopathy (CAA), a common type of cerebral small vessel disease (SVD) defined by the cerebrovascular accumulation of amyloid-β, has become one of the important contributors of age-related cognitive impairment and dementia.[1,2] SVD neuroimaging markers including lobar cerebral microbleeds (CMB), cortical microinfarcts (CMI), multiple subcortical white matter hyperintensity spots (WMH), lobar lacunes of presumed vascular origin (lacunes), enlarged centrum semiovale perivascular spaces (CSO-PVS), and cortical superficial siderosis (cSS) constitutes key features in its diagnosis.[3] Studies have shown that neuropsychiatric symptoms are prevalent in individuals with SVD and are promising preclinical indicators of early disease progression.[4] However, most studies on SVD-related neuropsychiatric symptoms had been focused on the non-CAA population.[4]

The distinct pathological distribution and mechanisms of CAA from other SVDs necessitate a bespoke investigation to discover neural mechanisms and imaging correlates of neuropsychiatric symptoms in CAA.[1] These understandings are crucial for future development of appropriate management and targeted treatments aimed to prevent and reverse disease progression.[4]

Apathy, defined as lack of motivation and a reduction in goal-directed behaviours,[5] has been reported as the most common neuropsychiatric symptoms in patients with CAA.[6] Current understanding of the neural mechanisms underlying apathy points to a disruption in the fronto-striatal circuit (the reward network)[5] – a network of brain regions regrouping the anterior cingulate cortex, the orbitofrontal cortex, the ventral striatum, and the ventral pallidum. Evidence from other neurodegenerative diseases and SVD have shown a link between apathy symptoms and a decrease in gray matter volume[5,7] and functional changes[8-10] within the reward network. Furthermore, apathy symptoms were also found to be correlated with SVD neuroimaging markers, particularly white matter hyperintensity (WMH) severity and the number of lacunes, in patients with non-CAA SVD.[4]

Advanced neuroimaging technique such as diffusion tensor imaging (DTI) has allowed detection of white matter microstructural damage beyond those identifiable on conventional MRI, which is useful in CAA where white matter is invariably affected. In fact, a few DTI studies in non-CAA SVD have revealed that apathy symptoms were related to extensive white matter tract disruptions in the reward network.[11,12] On the other hand, resting-state functional MRI is considered an essential tool for assessing neural correlates of a symptom or a behaviour beyond the observable structural changes. Indeed, aberrant functional connectivity in key hubs within the fronto-striatal reward circuit has been shown to be associated with apathy symptoms in patients with Alzheimer's disease and Parkinson's disease.[8-10]

At present, the characteristics and neural mechanisms of apathy in CAA are largely unexplored. This study aimed to assess the prevalence, clinical characteristics, and neural underpinnings of apathy in a pure CAA cohort. Apathy was assessed using the Apathy Scale which interrogated the whole range of apathy symptoms. We also acknowledged that although apathy shares many overlapping symptoms with depression, several studies have supported their distinct neural correlates.[11,13-15] Therefore, we attempted to discern the effect of depression from apathy in our analyses. To determine the underlying neural mechanisms contributing to apathy symptoms, we employed a multi-modal neuroimaging approach incorporating SVD neuroimaging markers, volumetric brain analysis (VBM of the gray

matter), DTI, and resting-state functional MRI. We hypothesized that apathy would be associated with a disruption to white matter connections in the fronto-striatal reward circuit represented by measured DTI parameters and to overall CAA pathology intrinsically related to SVD neuroimaging markers. We further hypothesized that a reduced gray matter volume and aberrant connectivity involving key hubs in the reward circuit could contribute to symptoms of apathy in CAA.

Materials and methods

This study was approved by the Institutional Review Board of the Massachusetts General Hospital, and written informed consents were obtained from all subjects or their surrogates according to the Declaration of Helsinki.

Study design

This is a cross-sectional study of an ongoing prospective single-center memory clinic research cohort from the Massachusetts General Hospital.

Study participants

Participants presenting with cognitive symptoms were recruited between March 2015 and December 2020. The inclusion criteria were: 1) diagnosis of probable CAA by modified Boston criteria (≥ 2 hemorrhagic lesions restricted to lobar, cortical, or cortical-subcortical regions or single hemorrhagic lesion and cortical superficial siderosis (cSS) and age ≥ 55) and 2) no contraindication for an MRI scan. Participants diagnosed with dementia (Mini-Mental State Examination (MMSE) ≤ 24 and/or impairment of instrumental activities of daily living) and participants with a history of symptomatic intracranial hemorrhage or macrohemorrhagic lesion on MRI were excluded.

Demographic and clinical data were collected from each participant upon enrollment. All participants then underwent a detailed neuropsychological evaluation and a research brain MRI.

Neuropsychological evaluation

The MMSE was used to assess global cognition. A battery of standardized cognitive tests was used to assess cognitive function in each domain as previously described in Schoemaker et al.[16] Briefly, the following domains were assessed: 1) executive function, 2) attention/processing speed, 3) memory, 4) language/semantics and 5) visuospatial functions. Raw scores from each test were transformed into z-scores and adjusted for age and education based on published normative data. Adjusted z-scores of tests in each domain were averaged to get the composite z-score for the domain.

Apathy was measured using the Apathy Scale, which has been validated in patients with neurodegenerative disease. The scores range from 0 to 42.[17] Subjects with scores of 14 or higher were considered apathetic.[17]

Depression was measured using the 30-item Geriatric Depression Scale, with scores ranging from 0 – 30.[18] Several items on the Geriatric Depression Scale overlap with symptoms of apathy. To obtain a "pure" measure of depression, we excluded six items that were previously shown to reflect apathy from the Geriatric Depression Scale.[19] This allowed us to obtain a "GDS-depression" score, with a maximum score of 24. As depression often co-occurs with apathy, we used the GDS-depression score as a covariate in our analyses to dissociate the effect of depression from apathy.

Neuroimaging analyses

MRI acquisition

Images were obtained with a 3T MRI scan (Siemens Healthcare, Magnetom Prisma-Fit) using a 32-channel head coil at the Massachusetts General Hospital (Boston, USA). MRI sequences included a T1-weighted sagittal multiecho magnetization-prepared rapid acquisition with gradient echo (MPRAGE) (TR = 2,510 ms; TE = 1.69 ms; slice thickness =1 mm; in-plane resolution = 1 x 1 mm), a 3D fluid attenuated inversion recovery (FLAIR) (TR = 5000 ms; TE = 356 ms; slice thickness = 0.9 mm; in-plane resolution = 0.9 x 0.9 mm), a susceptibility-weighted imaging (TR = 30 ms; TE = 20 ms; slice thickness = 1.4mm; in-plane resolution = 0.86 x 0.86 mm), a high-resolution diffusion-weighted imaging (64 directions; TR = 8000 ms; TE = 82 ms; slice thickness = 2 mm; in-plane resolution = 2 x 2 mm; b-value

= 700 s/mm^2). Functional images were acquired during rest (46 axial slices; TR = 3000 ms; TE = 30 ms; slice thickness = 3 mm; in-plane resolution = 3 x 3 mm). The acquisition time was 6 minutes and 12 seconds. Participants were instructed to rest with their eyes open during the resting-state functional MRI acquisition.

Neuroimaging markers of cerebral small vessel disease

Conventional markers of SVD were rated by a neuroradiologist (MCZZ) blinded to clinical data, according to the Standards for Reporting Vascular Changes on Neuroimaging (STRIVE) recommendations.[20]

The number and location of the CMBs and the presence of cSS were evaluated on susceptibility-weighted images.[20] Lacunes were identified on FLAIR images.[20] CMIs were identified as lesions ≤ 4 mm, restricted to the cortex, hypointense on T1-weighted images, hyperintense on FLAIR images, and distinct from perivascular spaces.[21] The CSO-PVS was rated using the T1-weighted images according to a previously proposed scale: 0 (none); 1 (1-10); 2 (11-20); 3 (21-40); 4 (>40).[22]

The total brain volume and the estimated total intracranial volume were calculated using the FreeSurfer software (www.surfer.nmr.mgh.harvard.edu; version 6.0).[23] The normalized total brain volume was obtained by dividing the total brain volume by the estimated total intracranial volume.

WMH lesions were segmented on FLAIR images using the lesion prediction algorithm as implemented in the Lesion Segmentation Tool version 3.0.0 (www.statistical-modelling.de/lst.html) for Statistical Parametric Mapping 12 (SPM12).[24] The normalized WMH volume was obtained by dividing the WMH volume by the estimated total intracranial volume.

A composite score for SVD burden in CAA, the CAA-SVD score, was chosen as a tool to represent the overall SVD burden. The score was precomputed by awarding one point to each of the following MRI markers: lobar CMBs, cSS, moderate-to-severe CSO-PVS, and WMH (confluent deep WMH Fazekas score 2-3 or irregular periventricular WMH Fazekas 3). Two points were given for five or more lobar CMBs and for the presence of disseminated cSS, for a total CAA-SVD score ranging from zero to six.[25]

Structural MRI preprocessing and Voxel-based morphometry

We used the CAT12 toolbox (cat12, The Structural Brain Mapping Group, University of Jenna, Germany) implemented on the SPM12 software (Wellcome Centre for Human Neuroimaging, London, UK) to preprocess and analyze the 3D T1-weighted images.[26] First, all 3D T1-weighted images were denoised, bias-corrected, affine-registered, and subsequently segmented into gray matter, white matter, and CSF. The segmented tissues were then spatially normalized to a common reference space using Shooting registration.[27] Next, the images' visual inspection and sample homogeneity test were done to check for segmentation errors, artifacts, and outliers. Finally, all images were smoothed using a 6-mm full width at half maximum (FWHM) Gaussian kernel.

Whole-brain voxel-based gray matter analysis was performed on SPM12 using the general linear model to test for group effect (apathetic vs. non-apathetic group) with an initial uncorrected two-tailed voxel-wise threshold of $p < 0.001$. An absolute masking of 0.05 was used to avoid edge effects around the border between the gray and white matter. Total intracranial volume, age, gender, and GDS-depression were added as covariates. A mask of regions of interest in the fronto-striatal circuit known to be associated with apathy was created using the built-in neuromorphometrics atlas in CAT12. The mask comprised bilateral accumbens, pallidum, anterior cingulate gyrus, gyrus rectus, and medial frontal cortices. A small volume correction within the pre-specified mask was performed and cluster(s) with a two-tailed cluster-level family-wise error corrected p (p_{FWE}) < 0.05 will be reported.

Diffusion tensor imaging preprocessing and analysis

All diffusion weighted images were visually inspected, and cases with excessive head motion or susceptibility artifacts were excluded. Briefly, the preprocessing steps included denoising,[28] removal of Gibbs Ringing Artifacts,[29] brain extraction,[30] and eddy current distortion and motion correction using the ‘eddy’ tool from the Functional Magnetic Resonance Imaging of the Brain Software Library (FSL) version 5.0.10.[31] The FSL’s ‘dtifit’ command was used for tensor fitting and calculation of scalar diffusion parameters (i.e., median diffusivity and fractional anisotropy).[32]

Voxel-wise statistical analysis of the median diffusivity and fractional anisotropy data was carried out using Tract-Based Spatial Statistic[33]. Briefly, all subject's fractional anisotropy data were registered to a common space (FMRIB58_FA standard-space) and averaged to create a mean fractional anisotropy map, which was then used to generate a tract skeleton, thresholded at fractional anisotropy > 0.2. Next, the fractional anisotropy images from each participant were projected onto the mean fractional anisotropy skeleton, creating skeletonized fractional anisotropy maps used for voxel-wise statistics. Similar analysis of the median diffusivity data was carried out by projecting the median diffusivity maps onto the mean fractional anisotropy skeleton. A general linear model comparing the fractional anisotropy and median diffusivity between the apathetic and the non-apathetic groups, controlling for age, gender, and GDS-depression, was conducted using the 'randomise' command to run the permutation-based nonparametric analysis with 5,000 iterations. Clusters with a two-sided threshold-free cluster enhancement (TFCE) $p < 0.05$, controlling for familywise error rate ($\alpha = 0.05$), were reported. Finally, tracts were identified using the standard Johns-Hopkins University DTI-based white-matter probability maps from the FSL toolbox.[34]

Resting-state functional MRI preprocessing and seed-based connectivity analysis

Preprocessing of resting-state functional MRI images was done using the CONN toolbox (version 20.b) (www.nitrc.org/projects/conn) implemented on the SPM12 software.[35] All images were preprocessed using the standard pipeline for functional image preprocessing. Briefly, realignment and motion correction, slice-timing correction, outlier identification, segmentation, and normalization into Montreal Neurological Institute space were applied to the images. Visual inspection of the preprocessed image was done for quality control. Smoothing with an 8 FWHM Gaussian kernel was applied. Finally, preprocessed images were denoised by regressing out the signal from confounder variables using the aCompcor approach[36] (noise from white matter and CSV, motion, outlier scans, and session effects), linear detrending, and by applying a temporal band-pass filter between 0.008 – 0.09 Hz.

Brain region(s) from VBM that demonstrated a significantly decreased volume in the apathetic compared to the non-apathetic group was chosen as seed(s) for the resting-state functional MRI analysis. Precisely, peak Montreal Neurological Institute coordinates of each

area of significant group differences identified using VBM were extracted, and a 10-mm diameter sphere was drawn around these coordinates to create a region of interest. Maps of significant correlations between the spherical seed region(s) and the rest of the brain was computed for the apathetic and the non-apathetic group separately using a seed-to-voxel approach. Obtained maps were then contrasted between groups using a general linear model, controlling for age, gender, and GDS-depression. Significant group differences between seed-to-voxel correlation maps were identified using a voxel-wise threshold of uncorrected two-tailed p-value < 0.001 and a cluster-size two-tailed familywise error corrected threshold of $p < 0.05$.

Statistical analysis

The Shapiro-Wilk test was used to assess for normal distribution of continuous variables. Demographics and clinical data between groups were compared using T-test for parametric continuous variables, Mann-Whitney U test for non-parametric variables, and chi-square test for dichotomous variables. Multiple linear regression analyses were used to assess the association between SVD neuroimaging markers and the Apathy Scale score. The Apathy Scale was entered as a dependent variable and each SVD neuroimaging marker was assessed separately as an independent variable. All neuroimaging markers were standardized before inputting into the model. Age, gender, and GDS-depression score were entered as covariates for all models. Sensitivity analyses excluding GDS-depression scores from the covariates were done (models with only age and gender as covariates). A complete case analysis was employed for all analyses. The number of missing data in each analysis were reported. A two-tailed p-value of < 0.05 was considered statistically significant. Data were analyzed using Python (v3.8.5) software.

Data availability

The data that supported the findings of this study are available on request from the corresponding author.

Result

Clinical and demographic data

Group differences on clinical and demographic variables are summarized in Table 1. Among the 37 participants with probable CAA, 16 were classified as apathetic and 21 as non-apathetic. There was no difference in age, gender, education, comorbid disease, or cognitive scores between the apathetic and the non-apathetic groups. Of note, all eight participants who had a score on the Geriatric Depression Scale suggestive of depression were in the apathetic group, constituting half of the apathetic group. While the GDS-depression scores, which isolates depressive symptoms from symptoms of apathy, showed a non-significant difference between the two groups, a trend towards a higher score in the apathetic group was observed (p=0.052). Accounting for one missing data on acetylcholine use in the apathetic group, no group difference was found.

Association of apathy with SVD neuroimaging markers

Group comparison across conventional MRI markers of SVD showed a significantly higher total CAA-SVD score and CSO-PVS score in the apathetic group. A trend toward a higher number of lobar CMBs in the apathetic group was found. There was no significant group difference in the other SVD neuroimaging markers (Table 1).

Multiple linear regression controlling for age, gender, and GDS-depression revealed the total CAA-SVD score as the only neuroimaging marker associated with scores on the Apathy Scale (standardized beta = 1.35 (0.07 – 2.62), p = 0.04, adjusted R^2 = 27.90%, F = 4.48), as shown in Table 2. The result of sensitivity analyses excluding GDS-depression score from the covariates showed no significant association between SVD neuroimaging marker and the Apathy Scale (eTable 1 in online supplemental material).

Voxel-based morphometry

A test for the difference in voxel-wise gray matter volume between the apathetic and non-apathetic groups within the pre-specified regions of interest revealed a significant decrease in gray matter volume of the bilateral orbitofrontal cortices, after controlling for age, gender, GDS-depression score, and total intracranial volume, F = 13.20, $p_{uncorrected} < 0.001$ based on the peak coordinate, cluster-size family-wise error corrected p = 0.028 (Figure 1).

Diffusion imaging and tract-based spatial statistic

Thirty-three out of the initial thirty-seven participants - 15 apathetic and 18 non-apathetic - had a complete DTI study. There was no significant group difference in

demographic, clinical, cognitive, or neuroimaging characteristics between those who completed the study and those who did not in both groups.

The apathetic group demonstrated lower fractional anisotropy in several tracts compared to the non-apathetic group after controlling for age, gender, and GDS-depression, pTFCE < 0.05 (Figure 2A). Analysis of the local maxima showed the most significant fractional anisotropy reduction in the bilateral inferior fronto-occipital fasciculus, the forceps minor, the bilateral superior longitudinal fasciculus, the left inferior longitudinal fasciculus, the bilateral corticospinal tract, and the right anterior thalamic radiation (eTable 2 in online supplemental material). To a lesser extent, we found higher median diffusivity in the right superior longitudinal fasciculus and the right anterior thalamic radiation in the apathetic group than the non-apathetic group, pTFCE < 0.05 (Figure 2B, eTable 2 in online supplemental material).

Resting-state functional MRI seed-based analysis

Thirty-six subjects were included in the fMRI analysis; one subject from the apathetic group was excluded due to an incomplete fMRI acquisition.

Using the orbitofrontal cortex region of interest (from VBM analysis) as a seed, we did not find any significant areas that differ in the resting-state functional connectivity between the apathetic and the non-apathetic group after controlling for age, gender, and GDS-depression.

Discussion

In our memory-clinic CAA cohort, the observed prevalence of apathy of was 43%, which is comparable to those reported in other CAA[6] and non-CAA SVD (arteriosclerosis[11,14] and cerebral autosomal dominant arteriopathy with subcortical infarcts and leukoencephalopathy (CADASIL) [37,38]). Crucially, the findings in this study demonstrated that apathy in CAA was underpinned by distinct neural structural change in the fronto-striatal circuit reward network. Within the reward circuit, the orbitofrontal cortex emerged as a key region associated with apathy symptoms across the multi-modal imaging studies. Extensive white matter microstructural disruption in the apathetic group relative to the non-apathetic group further supported a link between symptoms of apathy and the disconnections between brain regions.

Le Heron et al.[5] had proposed a framework for understanding the underlying processes leading to symptoms of apathy. The framework described the three key phases of a normal motivated behaviour: 1) the cost-benefit evaluation of whether to perform an action or a series of actions, 2) performing and persisting with the behaviour, and 3) learning and remembering rewarding behaviours. Consequently, an impairment in any of these processes could result in a reduction in goal-directed behaviour and apathy.

The orbitofrontal cortex was proposed to be involved in the first phase of evaluating the reward value.[39] Reduced reward sensitivity has been shown to underlie the altered effort-based decision-making process in apathy in both stroke and Parkinson's disease.[40,41] As a hub that receives afferent connections of ventral streams from all sensory modalities – visual, taste, olfactory, somatosensory, and auditory; the orbitofrontal cortex is able to portray a multi-modal representation of each stimulus and provide an accurate determination of the reward value.[39] In fact, functional and structural changes in the orbitofrontal cortex have been shown to relate to apathy in a wide range of neurodegenerative diseases, including Alzheimer's disease, frontotemporal dementia, and Parkinson's disease.[5,42,43]

Another key finding in our study was the extensive involvement of white matter tracts found to be associated with apathy, independent of depression, which corroborated the concept of apathy as a disconnection syndrome. Afferent and efferent pathways connecting regions within the reward network were postulated to play an instrumental role in facilitating the processes involved in effort-based decision-making and goal-directed behaviour. Essentially, information from afferent sensory regions and emotional information are integrated and passed on to areas performing cost-benefit evaluation and decision-making. These decisions and execution plans must be conveyed to effector regions to instigate actions, while the feedback of perceived reward values, in turn, influence the maintenance and modification of successive behaviours.

Certain white matter tracts shown to be associated with apathy in our study constitute key pathways in processes associated with generation of goal-directed behaviours. The importance of effective communication between sensory regions and frontal areas was exemplified here by the involvement of two major pathways linking the visual cortex to the frontal lobe in the apathetic group, namely, the inferior longitudinal fasciculus and the inferior fronto-occipital fasciculus. Notably, the inferior fronto-occipital fasciculus had also been previously implicated with apathy symptoms in non-CAA SVD and frontotemporal dementia.[11,12,43]

Another important tract identified to be associated with apathy in our study was the forceps minor, which is the main tract that connects the bilateral orbitofrontal cortices and the prefrontal regions.[44] These regions are responsible for both emotional/motivational and cognitive aspects of executive function including the integration of emotion and social context for decision making, planning and execution of movements.[45] Therefore, it's been suggested that a compromised connection between the bilateral prefrontal regions may result in apathy through poor decision making and impaired motor processing.[46] Indeed, studies in neurodegenerative diseases and SVDs have confirmed the association of the integrity of the forceps minor and other parts of the corpus callosum with apathy.[5,11,12,42,43]

Association pathways connecting frontal and other cortices also play a significant role in supporting the execution of goal-directed behaviours. Notable tracts from our result included the anterior thalamic radiation and the superior longitudinal fasciculus. The anterior thalamic radiation connects the frontal lobe to the thalamus and the limbic systems. In addition to being the main pathway connecting frontal and subcortical structures, it is also considered a prominent component of the emotion regulation process.[47] Findings of apathy in both SVD and CADASIL, a genetic form of SVD, supported a correlation between lower white matter integrity in the anterior thalamic radiation and a higher degree of apathy.[11,12,38] Likewise, the superior longitudinal fasciculus was found to be associated with apathy in studies in amnestic mild cognitive impairment and progressive supranuclear palsy.[46,48] Its role in the spatial attention network was suggested to complement the generation of goal-directed behaviours.[46]

Finally, the role of projection fibres to the effector regions in the initiation and maintenance of actions and behaviours should not be overlooked. The corticospinal tract is considered one of the core pathways conveying sensorial information and motor commands to the subcortical nuclei. The association observed between decreased microstructural integrity in the corticospinal tracts and apathy in our study matched findings in patients with amnestic cognitive impairment.[46]

Interestingly, our analysis revealed the CAA-SVD score as the only significant SVD neuroimaging marker associated with apathy independent of depression. A trend toward a higher number of CMBs were also observed in the apathetic group compared to the non-apathetic group. These findings may indicate that apathy was more prevalent in patients with higher disease burden and corroborated the findings of the association between apathy and extensive disruption of white matter networks. Indeed, the CAA-SVD composite score had been shown to reliably reflect the underlying CAA-related vasculopathic change on

pathology, outperforming other single SVD markers.[25] A higher number of CMBs distributed throughout the cortical areas in the apathetic group might in part explain the widespread involvement of white matter damage demonstrated in the DTI analysis.

Few existing functional MRI studies have linked apathy to altered resting-state functional connectivity between components of the fronto-striatal circuit. Two notable studies in Parkinson's disease reported that patients with higher apathy had weaker resting-state functional connectivity between the striatum and the frontal brain regions, including the orbitofrontal cortex.[8,10] Another study in Alzheimer's disease have found altered resting-state functional connectivity associated with apathy in regions connected to the salience network.[9] Our result did not show any significant areas of altered resting-state functional connectivity connected to the orbitofrontal cortex in association with apathy in our population. However, we were likely underpowered by our small sample size. Future studies addressing resting-state functional connectivity changes associated with apathy in SVD are warranted to discern the functional connectivity changes related to apathy in these conditions.

By using a multi-modal neuroimaging approach, we were able to portray the underlying pathology in CAA captured through various measures through the different neuroimaging modalities. First, our results suggested that the structural disconnection of the brain regions in the reward circuits were significantly associated with symptoms of apathy in CAA. Our findings coincided with a proposal by Tay et al.[13] that apathy is a consequence of disruptions to large-scale white matter networks in SVD. Secondly, the orbitofrontal cortex and its connection to other key regions in the reward circuit were centrally related to apathy. Thirdly, we found that the degree of apathy in CAA correlated with the severity of the underlying CAA burden measured by the CAA-SVD composite score. Collectively, findings from our multi-modal neuroimaging analysis enabled a comprehensive understanding of the underlying neurological underpinnings of apathy in CAA.

The main strength of our study was the use of multi-modal neuroimaging techniques to capture different neural correlates of apathy in CAA. Moreover, the use of a validated questionnaire for apathy rather than general screening questionnaires allowed a more detailed inspection of the different symptoms of apathy and improved sensitivity in apathy detection. In addition, it allowed distinction of symptoms of apathy from depression, albeit the delineation was practically not absolute. Finally, as CAA pathology is more prevalent in the elderly and was shown to be associated with cognitive impairment and dementia,[49] our findings could potentially contribute to the development of novel treatments for neuropsychiatric symptoms in CAA and other neurodegenerative diseases.

There are several limitations to this study. Firstly, to mitigate confounding, we had limited our population to the non-demented CAA population presenting without ICH. Caution should be taken when interpreting and generalising our findings to other CAA phenotypes. Secondly, it is not possible to assume a causal relationship between apathy and structural or functional changes due to the cross-sectional study design, future studies should employ a longitudinal study design to address this. Thirdly, our small sample size and lack of a control (non-CAA) group may have limited our power to detect neural and clinical correlates and exposed the analyses to risk of model overfitting. Therefore, replication of our study in larger samples with a control group is warranted. Finally, our measurement of apathy is self-rated and therefore is subject to the perception and insight of the informant. Objective measurement of apathy or task-based analysis might yield more accurate results.

Conclusion

Our result revealed that apathy was prevalent in CAA and a higher CAA burden correlated to a higher degree of apathy. Furthermore, symptoms of apathy in CAA were underpinned by disruption to the fronto-striatal reward circuit, particularly the involvement of the orbitofrontal cortex. Most importantly, microstructural damage in white matter tracts and disintegration of their connections emerged as a preeminent factor associated with the neural mechanisms of apathy in CAA.

WNL-2023-000097_etab --- http://links.lww.com/WNL/C702

References

1. Charidimou A, Boulouis G, Gurol ME, et al. Emerging concepts in sporadic cerebral amyloid angiopathy. *Brain*. Jul 1 2017;140(7):1829-1850. doi:10.1093/brain/awx047
2. Zanon Zotin MC, Sveikata L, Viswanathan A, Yilmaz P. Cerebral small vessel disease and vascular cognitive impairment: from diagnosis to management. *Curr Opin Neurol*. Apr 1 2021;34(2):246-257. doi:10.1097/WCO.0000000000000913
3. Charidimou A, Frosch MP, Al-Shahi Salman R, et al. Advancing diagnostic criteria for sporadic cerebral amyloid angiopathy: Study protocol for a multicenter MRI-pathology validation of Boston criteria v2.0. *Int J Stroke*. Dec 2019;14(9):956-971. doi:10.1177/1747493019855888
4. Clancy U, Gilmartin D, Jochems ACC, Knox L, Doubal FN, Wardlaw JM. Neuropsychiatric symptoms associated with cerebral small vessel disease: a systematic review and meta-analysis. *Lancet Psychiatry*. Mar 2021;8(3):225-236. doi:10.1016/S2215-0366(20)30431-4
5. Le Heron C, Apps MAJ, Husain M. The anatomy of apathy: A neurocognitive framework for amotivated behaviour. *Neuropsychologia*. Sep 2018;118(Pt B):54-67. doi:10.1016/j.neuropsychologia.2017.07.003
6. Smith EE, Crites S, Wang M, et al. Cerebral Amyloid Angiopathy Is Associated With Emotional Dysregulation, Impulse Dyscontrol, and Apathy. *J Am Heart Assoc*. Nov 16 2021;10(22):e022089. doi:10.1161/JAHA.121.022089
7. Kumfor F, Zhen A, Hodges JR, Piguet O, Irish M. Apathy in Alzheimer's disease and frontotemporal dementia: Distinct clinical profiles and neural correlates. *Cortex*. Jun 2018;103:350-359. doi:10.1016/j.cortex.2018.03.019
8. Baggio HC, Segura B, Garrido-Millan JL, et al. Resting-state frontostriatal functional connectivity in Parkinson's disease-related apathy. *Mov Disord*. Apr 15 2015;30(5):671-9. doi:10.1002/mds.26137
9. Jones SA, De Marco M, Manca R, et al. Altered frontal and insular functional connectivity as pivotal mechanisms for apathy in Alzheimer's disease. *Cortex*. Oct 2019;119:100-110. doi:10.1016/j.cortex.2019.04.008
10. Lucas-Jimenez O, Ojeda N, Pena J, et al. Apathy and brain alterations in Parkinson's disease: a multimodal imaging study. *Ann Clin Transl Neurol*. Jul 2018;5(7):803-814. doi:10.1002/acn3.578
11. Hollocks MJ, Lawrence AJ, Brookes RL, et al. Differential relationships between apathy and depression with white matter microstructural changes and functional outcomes. *Brain*. Dec 2015;138(Pt 12):3803-15. doi:10.1093/brain/awv304
12. Saleh Y, Le Heron C, Petitet P, et al. Apathy in small vessel cerebrovascular disease is associated with deficits in effort-based decision making. *Brain*. May 7 2021;144(4):1247-1262. doi:10.1093/brain/awab013
13. Tay J, Tuladhar AM, Hollocks MJ, et al. Apathy is associated with large-scale white matter network disruption in small vessel disease. *Neurology*. Mar 12 2019;92(11):e1157-e1167. doi:10.1212/WNL.0000000000007095
14. Lohner V, Brookes RL, Hollocks MJ, Morris RG, Markus HS. Apathy, but not depression, is associated with executive dysfunction in cerebral small vessel disease. *PLoS One*. 2017;12(5):e0176943. doi:10.1371/journal.pone.0176943
15. Douven E, Staals J, Freeze WM, et al. Imaging markers associated with the development of post-stroke depression and apathy: Results of the Cognition and Affect after Stroke - a Prospective Evaluation of Risks study. *Eur Stroke J*. Mar 2020;5(1):78-84. doi:10.1177/2396987319883445

16. Schoemaker D, Charidimou A, Zanon Zotin MC, et al. Association of Memory Impairment With Concomitant Tau Pathology in Patients With Cerebral Amyloid Angiopathy. *Neurology*. Apr 13 2021;96(15):e1975-e1986. doi:10.1212/WNL.0000000000011745
17. Starkstein SE, Mayberg HS, Preziosi TJ, Andrezejewski P, Leiguarda R, Robinson RG. Reliability, validity, and clinical correlates of apathy in Parkinson's disease. *J Neuropsychiatry Clin Neurosci*. Spring 1992;4(2):134-9. doi:10.1176/jnp.4.2.134
18. Yesavage JA, Brink TL, Rose TL, et al. Development and validation of a geriatric depression screening scale: a preliminary report. *J Psychiatr Res*. 1982;17(1):37-49. doi:10.1016/0022-3956(82)90033-4
19. Adams KB, Matto HC, Sanders S. Confirmatory factor analysis of the geriatric depression scale. *Gerontologist*. Dec 2004;44(6):818-26. doi:10.1093/geront/44.6.818
20. Wardlaw JM, Smith EE, Biessels GJ, et al. Neuroimaging standards for research into small vessel disease and its contribution to ageing and neurodegeneration. *Lancet Neurol*. Aug 2013;12(8):822-38. doi:10.1016/S1474-4422(13)70124-8
21. van Veluw SJ, Shih AY, Smith EE, et al. Detection, risk factors, and functional consequences of cerebral microinfarcts. *Lancet Neurol*. Sep 2017;16(9):730-740. doi:10.1016/S1474-4422(17)30196-5
22. Potter GM, Chappell FM, Morris Z, Wardlaw JM. Cerebral perivascular spaces visible on magnetic resonance imaging: development of a qualitative rating scale and its observer reliability. *Cerebrovasc Dis*. 2015;39(3-4):224-31. doi:10.1159/000375153
23. Fischl B. FreeSurfer. *Neuroimage*. Aug 15 2012;62(2):774-81. doi:10.1016/j.neuroimage.2012.01.021
24. Schmidt P. *Bayesian inference for structured additive regression models for large-scale problems with applications to medical imaging.* Ludwig-Maximilians-Universität München; 2017. http://nbn-resolving.de/urn:nbn:de:bvb:19-203731.
25. Charidimou A, Martinez-Ramirez S, Reijmer YD, et al. Total Magnetic Resonance Imaging Burden of Small Vessel Disease in Cerebral Amyloid Angiopathy: An Imaging-Pathologic Study of Concept Validation. *JAMA Neurol*. Aug 1 2016;73(8):994-1001. doi:10.1001/jamaneurol.2016.0832
26. Kurth F, Gaser C, Luders E. A 12-step user guide for analyzing voxel-wise gray matter asymmetries in statistical parametric mapping (SPM). *Nat Protoc*. Feb 2015;10(2):293-304. doi:10.1038/nprot.2015.014
27. Ashburner J, Friston KJ. Diffeomorphic registration using geodesic shooting and Gauss-Newton optimisation. *Neuroimage*. Apr 1 2011;55(3):954-67. doi:10.1016/j.neuroimage.2010.12.049
28. Veraart J, Fieremans E, Novikov DS. Diffusion MRI noise mapping using random matrix theory. *Magn Reson Med*. Nov 2016;76(5):1582-1593. doi:10.1002/mrm.26059
29. Kellner E, Dhital B, Kiselev VG, Reisert M. Gibbs-ringing artifact removal based on local subvoxel-shifts. *Magn Reson Med*. Nov 2016;76(5):1574-1581. doi:10.1002/mrm.26054
30. Smith SM. Fast robust automated brain extraction. *Hum Brain Mapp*. Nov 2002;17(3):143-55. doi:10.1002/hbm.10062
31. Andersson JLR, Sotiropoulos SN. An integrated approach to correction for off-resonance effects and subject movement in diffusion MR imaging. *Neuroimage*. Jan 15 2016;125:1063-1078. doi:10.1016/j.neuroimage.2015.10.019

32. Basser PJ, Mattiello J, LeBihan D. Estimation of the effective self-diffusion tensor from the NMR spin echo. *J Magn Reson B*. Mar 1994;103(3):247-54. doi:10.1006/jmrb.1994.1037
33. Smith SM, Jenkinson M, Johansen-Berg H, et al. Tract-based spatial statistics: voxelwise analysis of multi-subject diffusion data. *Neuroimage*. Jul 15 2006;31(4):1487-505. doi:10.1016/j.neuroimage.2006.02.024
34. Hua K, Zhang J, Wakana S, et al. Tract probability maps in stereotaxic spaces: analyses of white matter anatomy and tract-specific quantification. *Neuroimage*. Jan 1 2008;39(1):336-47. doi:10.1016/j.neuroimage.2007.07.053
35. Whitfield-Gabrieli S, Nieto-Castanon A. Conn: a functional connectivity toolbox for correlated and anticorrelated brain networks. *Brain Connect*. 2012;2(3):125-41. doi:10.1089/brain.2012.0073
36. Behzadi Y, Restom K, Liau J, Liu TT. A component based noise correction method (CompCor) for BOLD and perfusion based fMRI. *Neuroimage*. Aug 1 2007;37(1):90-101. doi:10.1016/j.neuroimage.2007.04.042
37. Jouvent E, Reyes S, Mangin JF, et al. Apathy is related to cortex morphology in CADASIL. A sulcal-based morphometry study. *Neurology*. Apr 26 2011;76(17):1472-7. doi:10.1212/WNL.0b013e31821810a4
38. Le Heron C, Manohar S, Plant O, et al. Dysfunctional effort-based decision-making underlies apathy in genetic cerebral small vessel disease. *Brain*. Nov 1 2018;141(11):3193-3210. doi:10.1093/brain/awy257
39. Rolls ET, Cheng W, Feng J. The orbitofrontal cortex: reward, emotion and depression. *Brain Commun*. 2020;2(2):fcaa196. doi:10.1093/braincomms/fcaa196
40. Muhammed K, Manohar S, Ben Yehuda M, et al. Reward sensitivity deficits modulated by dopamine are associated with apathy in Parkinson's disease. *Brain*. Oct 2016;139(Pt 10):2706-2721. doi:10.1093/brain/aww188
41. Rochat L, Van der Linden M, Renaud O, et al. Poor reward sensitivity and apathy after stroke: implication of basal ganglia. *Neurology*. Nov 5 2013;81(19):1674-80. doi:10.1212/01.wnl.0000435290.49598.1d
42. Kos C, van Tol MJ, Marsman JB, Knegtering H, Aleman A. Neural correlates of apathy in patients with neurodegenerative disorders, acquired brain injury, and psychiatric disorders. *Neurosci Biobehav Rev*. Oct 2016;69:381-401. doi:10.1016/j.neubiorev.2016.08.012
43. Sheelakumari R, Bineesh C, Varghese T, Kesavadas C, Verghese J, Mathuranath PS. Neuroanatomical correlates of apathy and disinhibition in behavioural variant frontotemporal dementia. *Brain Imaging Behav*. Oct 2020;14(5):2004-2011. doi:10.1007/s11682-019-00150-3
44. Catani M, Thiebaut de Schotten M. A diffusion tensor imaging tractography atlas for virtual in vivo dissections. *Cortex*. Sep 2008;44(8):1105-32. doi:10.1016/j.cortex.2008.05.004
45. Robinson H, Calamia M, Glascher J, Bruss J, Tranel D. Neuroanatomical correlates of executive functions: a neuropsychological approach using the EXAMINER battery. *J Int Neuropsychol Soc*. Jan 2014;20(1):52-63. doi:10.1017/S135561771300060X
46. Setiadi TM, Martens S, Opmeer EM, et al. Widespread white matter aberration is associated with the severity of apathy in amnestic Mild Cognitive Impairment: Tract-based spatial statistics analysis. *Neuroimage Clin*. 2021;29:102567. doi:10.1016/j.nicl.2021.102567
47. Niida R, Yamagata B, Niida A, Uechi A, Matsuda H, Mimura M. Aberrant Anterior Thalamic Radiation Structure in Bipolar Disorder: A Diffusion Tensor Tractography Study. *Front Psychiatry*. 2018;9:522. doi:10.3389/fpsyt.2018.00522

48. Agosta F, Galantucci S, Svetel M, et al. Clinical, cognitive, and behavioural correlates of white matter damage in progressive supranuclear palsy. *J Neurol*. May 2014;261(5):913-24. doi:10.1007/s00415-014-7301-3
49. Keage HA, Carare RO, Friedland RP, et al. Population studies of sporadic cerebral amyloid angiopathy and dementia: a systematic review. *BMC Neurol*. Jan 13 2009;9:3. doi:10.1186/1471-2377-9-3

Tables

Table 1 Comparison of demographics, comorbidities, cognitive scores, and neuroimaging markers between the apathetic and the non-apathetic groups

Characteristics	Apathetic (n=16)	Non-apathetic (n=21)
Demographic variables		
Age	71.09 (7.33)	74.96 (6.79)
Male [n (%)]	9 (56%)	13 (61.9%)
Years of Education	16.38 (3.01)	17.29 (2.49)
Clinical variables		
Apathy Scale[1]	16.19 (2.40)	8.76 (2.53)
Geriatric depression scale [median (IQR)]	9 (4 - 15)	4 (2 - 5)*
GDS-depression [median (IQR)]	6.5 (2 - 11.25)	3 (2 - 4)
Hypertension [n (%)]	9 (56%)	14 (66.7%)
Hyperlipidemia [n (%)]	10 (62.5%)	17 (81%)
Diabetes [n (%)]	2 (12.5%)	3 (14.3%)
Atrial fibrillation [n (%)]	1 (6.2%)	1 (4.8%)
Acetylcholinesterase inhibitor [n (%)]	4 (26.6%)	4 (19%)
Cognitive variables		
Mini-mental state examination	28.00 (26 - 28.25)	27.00 (25 - 28)
Mini-mental state examination z-score	-0.54 (1.27)	-0.92 (1.32)
Attention processing speed [median (IQR)]	-0.28 (-0.57 - 0.37)	0.13 (-0.14 - 0.46)
Executive function [median (IQR)]	-0.23 (-1.14 - 0.22)	-0.26 (-0.83 - (-) 0.02)
Memory	-1.03 (1.36)	-1.27 (1.50)
Language [median (IQR)]	-0.22 (-1.30 - 0.47)	-0.41 (-0.95 - 0.04)
Visuospatial [median (IQR)]	0.22 (-0.63 - 1.00)	0.40 (-0.01 - 1.02)
MRI Markers of SVD		
Normalized total brain volume	0.64 (0.04)	0.62 (0.04)
Normalized WMH volume [median (IQR)]	0.0025 (0.0015 - 0.0087)	0.0027 (0.0009 - 0.0082)
Lobar cerebral microbleeds [median (IQR)]	63.5 (24.5 - 158)	11 (4 - 65)
Lobar lacunes [median (IQR)]	0 (0-0.5)	0 (0)
Cerebral microinfarct [median (IQR)]	0 (0 - 2)	0 (0 - 1)
CSO-PVS score [median (IQR)]	3 (3 - 4)	2 (2 - 4)*
Presence of cortical superficial siderosis [n (%)]	9 (56.3%)	7 (33.3%)
CAA-SVD score (IQR)	5 (3 - 6)	3 (2 - 4)*

Mean (standard deviation) are presented for each variable, unless otherwise indicated. For non-normally distributed data, median and interquartile range are presented. Scores on each cognitive domain are converted to z-scores before comparison.
*p-value < 0.05
[1] As the Apathy Scale was used to categorize the groups, we did not compare the Apathy Scale score between the groups.
CAA = cerebral amyloid angiopathy; CSO-PVS = centrum semiovale perivascular spaces; GDS = geriatric depression scale; IQR = interquartile range; WMH = white matter hyperintensity; SVD = cerebral small vessel disease.

Table 2 Multivariate regression analyses of the association between SVD neuroimaging markers and the Apathy Scale

Models	Standardized beta (95% CI)	Adjusted R^2 (%)	F-value
Base model			
Age, gender, GDS-depression		19.9	3.99*
SVD neuroimaging marker models: adjusted for age, gender, and GDS-depression scores			
Normalized WMH volume	0.67 (-0.74 – 2.08)	19.81	3.22*
Lobar cerebral microbleeds	0.94 (-0.39 – 2.26)	22.49	3.61*
Lobar lacunes	0.003 (-1.37 – 1.38)	17.44	2.90*
Cerebral microinfarct	-0.40 (-1.78 – 0.98)	18.32	3.02*
CSO-PVS score	0.69 (-0.68 – 2.06)	20.06	3.26*
Presence of cortical superficial siderosis	2.05 (-0.62 – 4.73)	23.31	3.73*
CAA-SVD score	1.35 (0.07 – 2.62)*	27.90	4.48*

The table summarizes the result from multivariate regression analyses investigating the association between SVD neuroimaging markers and apathy with the Apathy Scale as the dependent variable. The base model included only age, gender, and GDS-depression scores as independent variables. Each SVD neuroimaging marker model included the corresponding SVD neuroimaging marker as an independent variable in addition to age, gender and GDS-depression scores. Standardized regression coefficients and 95% confidence intervals (uncorrected for multiple comparisons) are shown for each neuroimaging marker except 'Presence of cortical superficial siderosis' (binary data) where the regression coefficients and 95% confidence interval are shown. The adjusted R squared values (percentage) and F-values are presented for the base model and for each SVD neuroimaging marker model.

*p-value < 0.05

Abbreviations: CAA = cerebral amyloid angiopathy; CI = confidence interval; CSO-PVS = centrum semiovale perivascular spaces; R2 = R squared; WMH = white matter hyperintensity; SVD = cerebral small vessel disease.

Figure Legends

Figure 1 Voxel-based morphometry analysis of gray matter volume between the apathetic and the non-apathetic groups (a whole-brain analysis with correction within a pre-specified reward network mask). The apathetic group showed reduced gray matter volume at the bilateral orbitofrontal cortex, family-wise error corrected cluster-size p = 0.028, number of voxels 131, MNI coordinates: -2, 39, -24. The color bar demonstrates F-value.

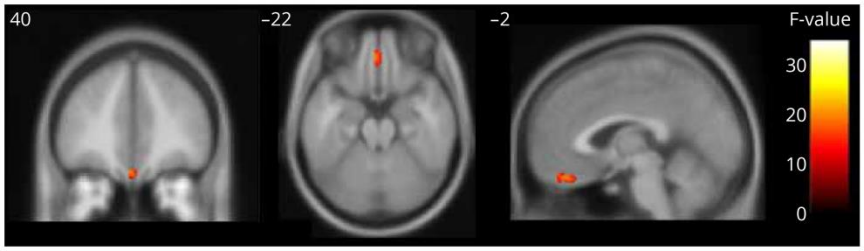

Figure 2 Tract-Based Spatial Statistic results comparing the FA and MD between the apathetic group and the non-apathetic group. Significant results with a threshold-free cluster enhancement (TFCE) p < 0.05 are displayed in red using the tbss_fill command. A) Displays white matter tracts with significantly lower FA in the apathetic group than the non-apathetic group. B) Displays white matter tracts with significantly higher MD in the apathetic group than the non-apathetic group. The results are overlayed on the mean FA skeleton (green). Significant clusters, peak p-value, MNI coordinates and their overlap with JHU White Matter Tractography atlas are shown in eTables 2 and 3 in online supplemental material.
ATR = anterior thalamic radiation; CST = corticospinal tract; FA = fractional anisotropy; IFOF = inferior fronto-occipital fasciculus; ILF = inferior longitudinal fasciculus; MD = median diffusivity; SLF= superior longitudinal fasiculus.

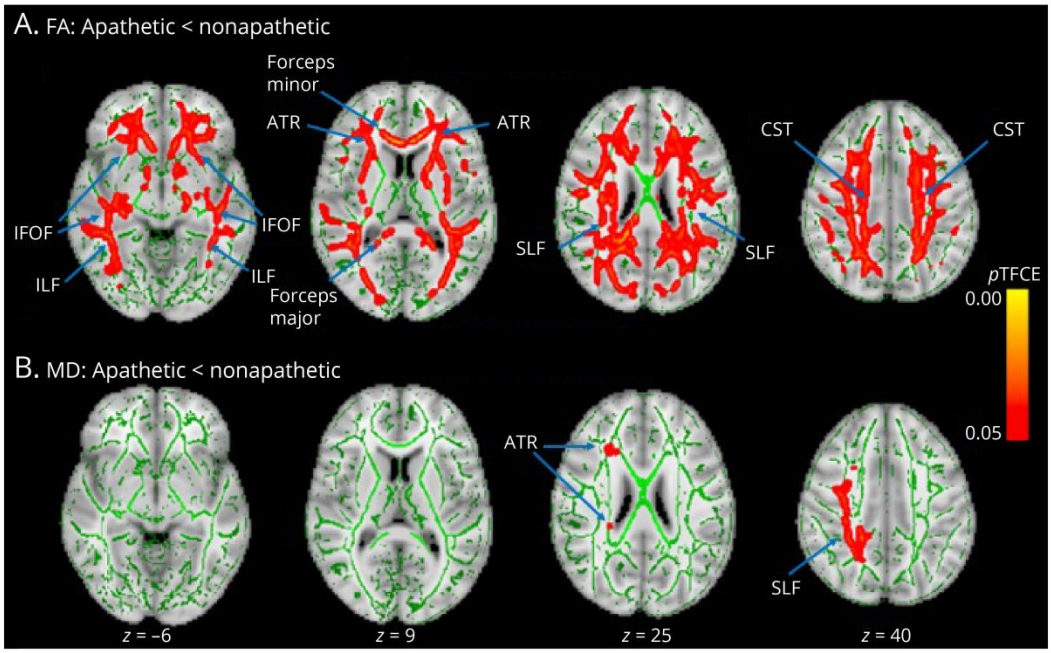

Apathy in Patients With Cerebral Amyloid Angiopathy: A Multimodal Neuroimaging Study

Anthipa Chokesuwattanaskul, Maria Clara Zanon Zotin, Dorothée Schoemaker, et al.

Neurology published online March 20, 2023
DOI 10.1212/WNL.0000000000207200